Clinical Neurophysiology 151 (2023) 50–58

Contents lists available at ScienceDirect

Clinical Neurophysiology

journal homepage: www.elsevier.com/locate/clinph

Directional recordings of somatosensory evoked potentials from the sensory thalamus in chronic poststroke pain patients

Andreas Nowacki [a,1,*], David Zhang [a,1], Jonathan Wermelinger [a,1], Pablo Abel Alvarez Abut [a], Jan Rosner [b,c], Claudio Pollo [a,2], Kathleen Seidel [a,2]

[a] Department of Neurosurgery, Inselspital, Bern University Hospital, University Bern, Bern, Switzerland
[b] Department of Neurology, Inselspital, Bern University Hospital, University Bern, Bern, Switzerland
[c] Spinal Cord Injury Center, Balgrist University Hospital, University of Zurich, Zurich, Switzerland

ARTICLE INFO

Article history:
Accepted 29 March 2023
Available online

Keywords:
Deep Brain Stimulation
Somatosensory evoked potentials
Neuropathic pain
Time–frequency analysis
High frequency components

HIGHLIGHTS

- A clear directionality of somatosensory evoked potentials recorded from segmented DBS leads in the sensory thalamus is observed.
- This directional effect provides further evidence in support of the somatotopy of the sensory thalamus.
- This may help identify the neurophysiological sweet spot in the possibly reorganized sensory thalamus in chronic pain patients.

ABSTRACT

Objective: The aim of this feasibility study was to investigate the properties of median nerve somatosensory evoked potential (SEPs) recorded from segmented Deep Brain Stimulation (DBS) leads in the sensory thalamus (**VP**) and how they relate to clinical and anatomical findings.
Methods: We analyzed four patients with central post-stroke pain and DBS electrodes placed in the **VP**. Median nerve SEPs were recorded with referential and bipolar montages. Electrode positions were correlated with thalamus anatomy and tractography-based medial lemniscus. Early postoperative clinical paresthesia mapping was performed by an independent pain nurse. Finally, we performed frequency and time–frequency analyses of the signals.
Results: We observed differences of SEP amplitudes recorded along different directions in the **VP**. SEP amplitudes did not clearly correlate to both atlas-based anatomical position and fiber-tracking results of the medial lemniscus. However, the contacts of highest SEP amplitude correlated with the contacts of lowest effect-threshold to induce paraesthesia.
Conclusions: SEP recordings from directional DBS leads offer additional information about the neurophysiological (re)organization of the sensory thalamus.
Significance: Directional recordings of thalamic SEPs bear the potential to assist clinical decision-making in DBS for pain.
© 2023 International Federation of Clinical Neurophysiology. Published by Elsevier B.V. This is an open access article under the CC BY license (http://creativecommons.org/licenses/by/4.0/).

1. Introduction

Deep brain stimulation (DBS) is an established therapy for several neurological diseases including chronic pain conditions such as central poststroke pain (CPSP) (Krauss et al., 2021). CPSP occurs after vascular lesions that typically affect the central somatosensory system. Among other targets, the sensory thalamus (ventral

* Corresponding author at: Department of Neurosurgery, Inselspital Bern University Hospital, University Bern, Bern, Switzerland.
E-mail address: neuro.nowacki@gmail.com (A. Nowacki).
[1] These authors contributed equally to this work and share the first authorship.
[2] These authors contributed equally to this work and share the last authorship.

https://doi.org/10.1016/j.clinph.2023.03.359
1388-2457/© 2023 International Federation of Clinical Neurophysiology. Published by Elsevier B.V.
This is an open access article under the CC BY license (http://creativecommons.org/licenses/by/4.0/).

posterior [VP] according to Hirai and Jones) has been most frequently stimulated to treat chronic neuropathic pain by evoking pleasant paresthesia in order to alleviate pain (Levy et al., 1987; Morel et al., 1997). After more than 50 years of its clinical application DBS for central pain remains a challenging procedure with highly variable outcomes ranging between 25–67% of responders (Katayama et al., 2001; Owen et al., 2006).

One contributing factor might be the difficulty to correctly target the sensory thalamus in these patients due to the limited delineation of the thalamic nuclei on magnetic resonance imaging (MRI) and high inter-individual functional segregation of the sensory thalamus especially in pain patients where functional reorganization can be expected (Lenz et al., 1998).

As a consequence, intraoperative neurophysiological examinations such as evoked potentials have been recognized as an increasingly important tool to characterize the "physiological" location of DBS electrodes and guide lead placement and postoperative contact selection (Lenz et al., 1998). The latest technological advancement with the introduction of segmented leads offers new opportunities to steer current into certain directions thereby providing further spatial restriction of the stimulation field to maximize the clinical effectiveness while reducing stimulation-induced side effects (Nguyen et al., 2020; Pollo et al., 2014). However, to our knowledge the feasibility to obtain directional somatosensory evoked potentials at the level of the sensory thalamus has not yet been investigated.

Thus, the aim of this study was to investigate the properties of median nerve somatosensory evoked potentials (SEPs) recorded form segmented leads placed within the sensory thalamus. We were interested if there are directional differences of thalamic SEPs and how these are related to the anatomical lead position and tractography findings of the medial lemniscal pathway. Furthermore, were interested in the frequency and time–frequency properties of these SEPs.

2. Methods

2.1. Patients and inclusion criteria

For the present study we included four patients (2 females, age ranging from 59 to 70 years) medication-refractory CPSP from of a larger cohort (n = 6) of which clinical data and outcomes were previously published (Nowacki et al., 2022). Directional somatosensory evoked potentials were not recorded in two out of six patients who were excluded from the present study. All patients fulfilled the criteria of definite CPSP according to established grading systems, and were clinically examined for dynamical mechanical (brush) allodynia and abnormal temperature sensibility (Klit et al., 2009). The distribution of subjective pain locations as well as individual findings for brush allodynia, altered temperature perception or heat- and cold-induced allodynia were mapped and documented on standardized pain drawings for each patient and sensory quality as previously published by our group (Nowacki et al., 2022). Patients' clinical characteristics are summarized in Table 1. In all patients, the DBS leads were placed in the sensory thalamus. All patients provided written and informed consent to the procedure and data analysis and the study was approved by the local institutional review board.

2.2. Surgical procedure and postoperative testing

Patients were operated under local anesthesia. Leads (8 contacts Boston Vercise Cartesia TM directional leads; Boston Scientific, U.S.A.) were implanted stereotactically using the Leksell-frame (Elekta, Sweden) targeting the sensory thalamus (VP) and central lateral thalamus (CL) as previously described (Nowacki et al., 2022) (Fig. 1). Fig. 2 displays the properties of the directional DBS lead. Contact 1 (dome tip contact surface area 6 mm^2, contact length 1.5 mm) and 8 (contact surface area 6 mm^2, contact length 1.5 mm) are ring contacts with contact 1 being the most distal. The middle two levels are segmented with three contacts 2/3/4 and 5/6/7 (segmented contact surface area 1.5 mm^2). There is a radiopaque marker that aligns with contacts 2 and 5. The outer diameter of the lead is 1.3 mm. Intraoperatively and on the first day after surgery, the electrodes were connected to an external pulse generator and patients were tested for occurrence of paresthesia and side-effects. To this end, each ring-level was tested in a bipolar mode with a fixed frequency of 50 Hz, 200 μs pulse width and increasing stimulation amplitudes starting from 0.5 mA to assess the stimulation threshold for paresthesia. We further tested individual directional contacts on the lead-level that yielded the lowest effect-threshold, again starting from 0.5 mA with 0.5 mA increments until paresthesia could be evoked. Paresthesia thresholds of each ring-mode and individual directional contact were obtained. After electrode implantation, leads were connected to extension cables and to an external pulse generator for 2–4 weeks. After this externalization phase patients decided to have their DBS electrodes connected to an internal pulse generator or – in case they did not profit from the stimulation – to have their DBS leads removed during a second operation under general anesthesia.

2.3. Electrode reconstruction and DTI-Tractography

We performed preoperative imaging with a 3-T MRI system (MAGNETOM Trio Tim, Siemens). A standard gadolinium-enhanced T1-weighted protocol (160 sagittal slices, 1-mm thickness) was followed by T2-weighted sequences (FOV 220 mm, acquisition matrix 128 × 128, repetition time (TR) 2000 msec, and multiple echo times (TE) values ranging from 12 msec to 96 msec in steps of 12 msec) and diffusion weighted imaging (DWI) with multishot echo-planar imaging (number of gradient directions 64, 1.8-mm slice thickness; 62 slices, TR 3300 msec, TE 64 msec, field of view 237 × 230 mm, b value 1000 sec/mm2). A postoperative high-resolution computed tomography (CT) scan was performed one day after surgery and fused to the preoperative MRI dataset and to reconstruct the electrode artifact with Brainlab Elements™ (Brainlab AG). Reconstructed electrodes were displayed in relation to fiber tracking results of the medial lemniscus. To this end, regions of interest were manually placed onto the primary sensory cortex and the posterior and lateral midbrain tegmentum posterior to the subthalamic nucleus (STN) and medial to the medial geniculate body as identifiable landmarks and setting tracking parameters to an FA-threshold of 0.2–0.3, 50 mm minimum length and 30° maximum angular deviation.

Lead orientation was inferred from intra- or postoperative fluoroscopy to determine the orientation of radio-opaque marker to deduce the direction of each individual directional contact. Reconstructed lead positions were projected onto the stereotactic atlas of Morel to correlate electrode positions with thalamus anatomy and patient-specific fiber-tracking results of the medial lemniscus. To this end, we used the vertical level (axial plane) between the two adjacent directional levels (level two and three) of the DBS lead. The corresponding atlas-level was used and projected onto each patient's individual MRI including the tractographic medial lemniscus reconstruction (Fig. 3).

2.4. Intraoperative recordings of SEPs with directional electrodes

SEP recordings were performed during the second stage of surgery (internalization of the implantable pulse generator [IPG] or explantation of the leads) under general anesthesia. Stimulation

Table 1
Demographic features, clinical characteristics, and key findings of SEP recordings and stimulation settings of the study cohort. C = contact; Cz = Central zero; VP = ventral posterior thalamus, MD/CL = mediodorsal/central lateral thalamus.

Patient	Sex	Age (years)	Stroke location	Predominant Pain Quality/ emotional pain rating	Objective Sensory Disturbances	Most efficient contact to induce paresthesia	Active Stimulation site at 12 months	Intraoperative VP. median nerve SEP recordings	Correlation with DTI
1	m	66	Lateral medualla oblongata	- burning, constant - distressing	Decreased warm and cold sensation, decreased brush sensation on contralateral face and arm	VP. thalamus: Contact **3+**, 6- at 1.5 mA	VP. thalamus: Contact 3+, 6-	Highest amplitudes between C1-**3** and C**3**-6 with clear phase reversal	Yes
2	f	70	Posterior thalamus	- heavy/ cramping/tender - shooting - horrible	Increased cold sensation, decreased brush sensation with mechanical allodynia on contralateral extremities (face excluded)	VP. thalamus: Contact **3-**, (5,6,7) + at 1 mA	Failed both MD/CL and VP. thalamus.	Highest amplitudes of Cz-6 and Cz-**3** and between C**3**-6	No
3	m	68	Lateral medualla oblongata	- burning, shooting - excrutiating	Decreased warm and cold sensation, decreased brush sensation on contralateral face, arm	VP. thalamus: Contact **3-**, (5,6,7) + at 1.0 mA	MD/CL: (5,6,7) -,8-; C+ VP. thalamus: (5,6,7) -,8-; C+	Highest amplitudes between Cz-6 and Cz-**3** and between C**3**-6	No
4	m	59	Lateral medualla oblongata	- burning, constant - horrible	Increased cold sensation and cold-allodynia, decreased brush sensation on contralateral hemi body (face excluded)	VP. thalamus: Contact **6**-, (2,3,4) + at 0.5 mA	MD/CL:1+, (2,3,4)-, (5,6,7) -, 8+ VP. thalamus: (5,6,7) -, 8+	Highest amplitudes between Cz-3 and Cz-4 and between C**6**-3	No

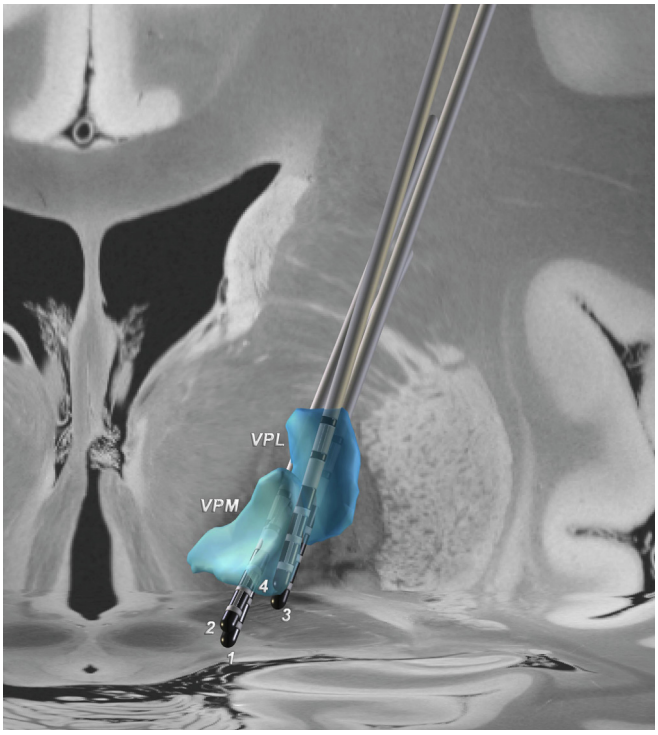

Fig. 1. Pseudo-3D projection of the implanted electrodes into the sensory thalamus (VP). Posterior, superior view with reconstructed electrodes of all four patients projected into a normalized human brain using LEAD-DBS. The blue area represents the ventral posterior thalamus (VP). Electrodes of patient 1 and 2 were implanted more medial and caudal in relation to the VP compared to patient 3 and 4. Medial part of the VP (VPM); lateral part of the VP (VPL).

for SEP of the median nerve was performed with an ISIS IOM System (Inomed, Emmendingen, Germany) using monopolar needles with a square wave pulse of 200 μs duration, rate of stimulation of 2.7 Hz and intensity of 10 – 25 mA. Recording was done with scalp cork screws electrodes located in Fz, Cź,Cʒ and Cʻ4, derived from international 10 – 20 system of electroencephalography (different montages were used, according to the signal-to-noise ratio) (MacDonald et al., 2019; Macdonald et al., 2007), with 100 – 150 averages, sweep of 50 – 100 ms, and sensitivity of 0.5 – 5 μV. The sampling frequency was 20,000 Hz and a hardware low-pass filter with a cut-off frequency of 5000 Hz was used. Further, we recorded responses to median nerve stimulation from the directional electrodes in the VP with monopolar and bipolar montages using a custom made adaptor to connect the DBS leads with the ISIS. Bipolar recordings were measured across contact 2 to 5, 3 to 6 and 4 to 7. For monopolar montages, each electrode (1–8) was measured with Cz as reference, except for patient 1, where contact 1 was used as a reference against contacts 2–7.

2.5. Frequency and time–frequency analysis

Neurophysiological data was analyzed off-line, using custom made Python 3 scripts. Recorded signals were cut to approximately 50 ms (1066 points) for comparability. We analyzed at least three different recordings of both monopolar and bipolar montages for each patient. The raw data was filtered to the following frequency bands, based on the segmentation applied by Pastor and Vega-Zelaya (Pastor and Vega-Zelaya, 2019):

- 20 – 300 Hz, corresponding to the range of low frequency components (LFC) (Note: we use a different terminology than Pastor et al., which will be discussed later)
- 500 – 1200 Hz, corresponding to the range of high frequency components (HFC)

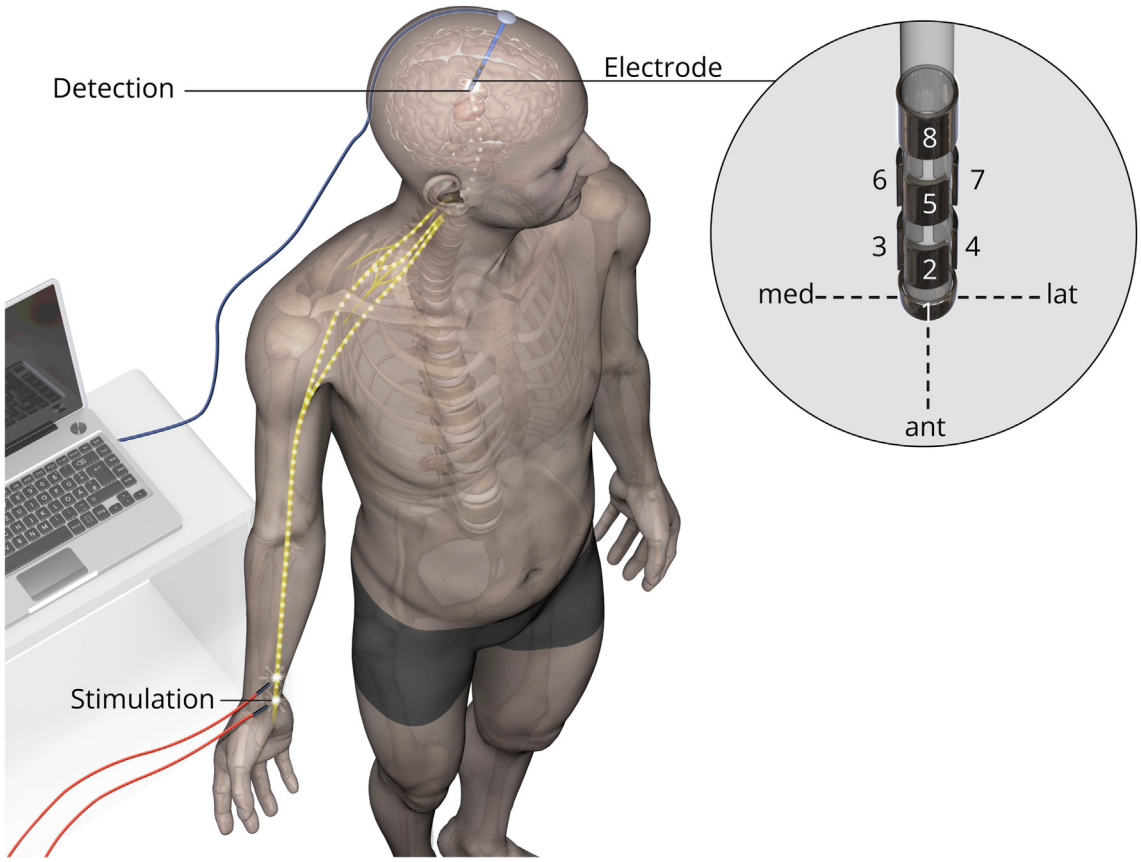

Fig. 2. Intraoperative set-up for somatosensory evoked potential (SEP) recordings from the Deep Brain Stimulation (DBS) lead. In this example, the segmented DBS lead was implanted into the left ventral posterior thalamus, which is connected to an external pulse generator. Intraoperatively, patients were given electrical stimuli from the contralateral median nerve using monopolar needles with a square wave pulse of 200 μs duration, rate of stimulation of 2.7 Hz and intensity of 10 – 25 mA. SEPs were recorded from the DBS lead with monopolar and bipolar montages. The properties of the segmented DBS lead highlighting the partial angular aperture is shown on the right: Contact 1 and 8 are ring electrodes with electrode 1 being the most distal. Contact 2/3/4 and 5/6/7 are directionally oriented from the two middle levels with each contact center being 120 degrees apart from each other.

- 1200 – 5000 Hz, corresponding to the range of the very high frequency components (VHFC)

In the following, we will use SEP amplitude and LFC amplitude interchangeably, since this approximately corresponds to the frequency band applied to monitor SEPs intraoperatively (usually 30–300 Hz) (MacDonald et al., 2019). A finite impulse response (FIR) filter with Kaiser window with 60 dB attenuation and a width of 0.007 = 700 Hz/NF where the Nyquist frequency (NF) is 10,000 Hz was applied (using the Python package *scipy.signal*). For all the different components, the amplitude (peak-to-peak) and the latency were determined. Following empirical optimization, the (onset) latency was determined as the time point when the filtered signal crossed the following quantity:

- $\begin{cases} M_b \pm 1\sigma \text{ for LFC} \\ M_b \pm 2.5\sigma \text{ for HFC and VHFC} \end{cases}$

minus 0.5 ms in the case of LFCs, and minus 1.0 ms in the case of HFCs and VHFCs. Here M_b is the mean of the baseline, defined as points 50 to 100 of the filtered signal, and σ is the standard deviation of the entire filtered signal. The latencies were double-checked visually and corrected if necessary. Furthermore, the main frequency of the HFC and VHFC was determined as the weighted average of the Fourier transform applied to the corresponding filtered signal. Finally, using a 1st order Gaussian derivative mother wavelet, a continuous wavelet transform of the raw signal was carried out (using the Python package *pywt*). The scalograms were plotted over the entire time frame and from 500 to 4000 Hz to capture the dynamics of the high and very high frequency components.

2.6. Statistics

Statistical analysis was done with IBM SPSS Statistics Version 28 and was restricted to signal analysis. Data was tested for normality distribution. A student's t-test was applied to compare means of two independent datasets and an ANOVA was applied if more than two groups were analyzed. These groups were mostly either the different patients, the different montages or the different quantities (latency, amplitude, etc.) separated according to frequency components (low, high, very high) within patients (see below). On SPSS, the "Split file" function was used before carrying out the statistical test, using multiple group levels according to what was being tested. For non-normally distributed data, we used the Kruskal Wallis test.

3. Results

3.1. Seps from directional DBS electrodes in the sensory thalamus

In all patients, we observed a clear directional effect of SEP amplitudes recorded from the DBS electrodes located in the sensory thalamus (Fig. 3). For monopolar recordings the neighboring directional contacts 3 or 6 showed the highest amplitude for median nerve SEP (**Supplementary Ta**bles 1 and 2**). Accordingly, the

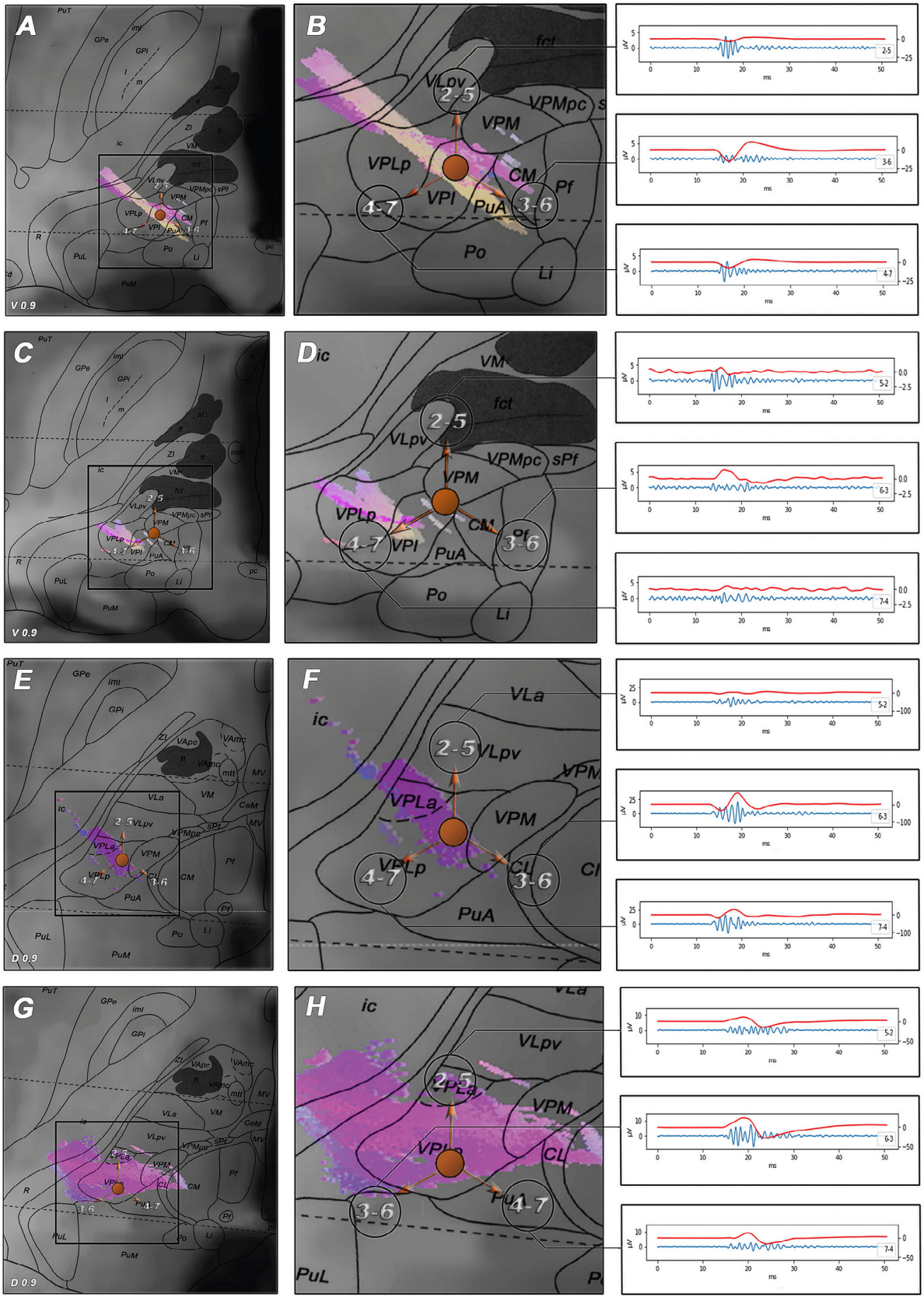
A
B
C
D ic
E
F
G
H
V 0.9
D 0.9
PuT
GPe
GPi
iml
ic
fct
VLpv
VPMpc
sPf
VPM
VPLp
CM
Pf
VPl
PuA
Po
Li
PuL
PuM
VLa
VPLa
CL
2-5
3-6
4-7
5-2
6-3
7-4
ms

bipolar montage of highest SEP amplitude was measured across contacts 3–6 for all four patients (Table 2).

3.2. Comparing SEP amplitudes to anatomical electrode position and tractography findings

In all patients, reconstructed electrodes projected onto the VP of the thalamus (Figs. 1 and 3). There was a certain variability in terms of the anatomical location of the stimulating electrode within the VP between patients, a finding that was expected due to adaptations of the definitive target point when considering the somatotopy in the VP to cover the painful area. More specifically, targets were chosen based on the main pain distribution: patients with primarily facial pain (patient 1) were implanted more medially in the medial part of the VP (VPM), whereas patients with a predominant extremity pain (patients 2 to 4) were implanted in the lateral part of the VP (VPL). Furthermore, electrodes projected onto the bulk of the tractography-based medial lemniscus. As can be inferred from Fig. 3, the size and shape of the bulk varied considerably between patients. Of note, in three out of four cases, the directional orientation of those individual electrodes with the highest SEP amplitudes did not point towards the center of gravity of the tractography-based medial lemniscus.

3.3. Comparing SEP amplitudes and paresthesia mapping

We found a correlation between the electrode contact of highest SEP amplitude and the contact of lowest effect-threshold to induce paresthesia during intraoperative clinical testing. As shown in Table 1, the most efficient contacts to induce paresthesia in the VP were also the contacts from which the highest SEP amplitudes (Table 2) were recorded during intraoperative median nerve stimulation. This was the case in all four patients.

3.4. Frequency and time–frequency analysis

The latencies, amplitudes and main frequencies of bipolar recordings for all patients are summarized in Table 3. Within patients, the following results were obtained. For patients 1 and 3, the latencies of LFCs, HFCs and VHFCs are significantly different ($p < 0.001$, ANOVA). The amplitude of HFCs and VHFCs are significantly different from the LFCs amplitude for patients 1 ($p = 0.005$, ANOVA), 2, and 4 ($p < 0.001$, ANOVA), but the amplitudes of the HFCs and VHFCs are not significantly different among themselves. Across patients, we observed the following. The latency and amplitude of LFCs, HFCs and VHFCs are all significantly different between patients ($p < 0.001$, Kruskal Wallis). Furthermore, the main frequency of the HFCs and VHFCs of patients 1 and 2 differ significantly from those of patients 3 and 4 ($p < 0.001$, ANOVA). Overall, patient 2 (thalamic infarct) had the lowest LFC amplitudes. Surprisingly, the amplitudes of the HFCs and VHFCs of patient 2 were higher than the LFC amplitude and similar to the HFC and VHFC amplitudes of patient 1.

Table 2
Comparison of mean amplitude (+/- standard deviation) of the different bipolar montages of all 4 patients. Standard deviation is based on 3 to 4 repetitive trials. LFC = low frequency component.

Amplitude (μV) of LFC	2–5	3–6	4–7
Patient 1	5.9 +/- 0.2	24.7 +/- 0.7	11.2 +/- 0.2
Patient 2	1.2 +/- 0.1	2.2 +/- 0.1	0.8 +/- 0.1
Patient 3	14.4 +/- 1.3	100.8 +/- 0.1	49.0 +/- 0.5
Patient 4	25.7 +/- 0.3	51.5 +/- 0.4	27.5 +/- 0.2

Table 3
Mean latencies, amplitudes and main frequencies (+/- standard deviation) of bipolar low frequency components (LFC), high frequency components (HFC) and very high frequency components (VHFC) of bipolar recordings of all 4 patients. Standard deviation is based on 3 to 4 repetitive trials.

	Latency (ms)	Amplitude (μV)	Main frequency (Hz)
Patient 1	LFC: 13.4 +/- 0.4	LFC: 14.0 +/- 8.4	
	HFC: 14.1 +/- 0.05	HFC: 5.7 +/- 2.1	HFC: 947.5 +/- 79.4
	VHFC: 14.3 +/- 0.2	VHFC: 7.2 +/- 2.1	VHFC: 2241.7 +/- 77.2
Patient 2	LFC: 13.2 +/- 0.5	LFC: 1.4 +/- 0.6	
	HFC: 13.7 +/- 1.7	HFC: 4.6 +/- 2.0	HFC: 967.9 +/- 62.6
	VHFC: 12.8 +/- 0.4	VHFC: 5.1 +/- 1.2	VHFC: 2211.7 +/- 90.8
Patient 3	LFC: 12.4 +/- 0.1	LFC: 54.7 +/- 37.7	
	HFC: 13.8 +/- 0.3	HFC: 29.6 +/- 9.4	HFC: 859.4 +/- 22.1
	VHFC: 13.5 +/- 0.4	VHFC: 26.0 +/- 10.7	VHFC: 2080.7 +/- 63.3
Patient 4	LFC: 15.2 +/- 0.9	LFC: 34.9 +/- 12.3	
	HFC: 15.2 +/- 0.2	HFC: 9.2 +/- 4.4	HFC: 871.0 +/- 37.7
	VHFC: 15.3 +/- 0.5	VHFC: 10.9 +/- 1.8	VHFC: 2020.5 +/- 89.6

The shape of the bipolar LFCs vary considerably from one patient to another (see Fig. 4). As for the HFCs and VHFCs, they come in bursts that are generally restricted to the duration of the LFC. Sometimes there appear to be two subsequent bursts (see Fig. 4, patient 1 HFC, patients 2 and 4 VHFC) or a single burst that diminishes over time (patient 3 HFC and VHFC). Most of the energy of HFC and VHFC seems to be concentrated in the upward deflection of the LFC (see Fig. 4). There do not appear to be separated areas of higher amplitude at any particular frequency, which might indicate that there are no lasting oscillations at any specific frequency (to be discussed in more detail below).

In patients 2, 3 and 4, the latency of the monopolar LFC, HFC and VHFC were significantly different from each other ($p < 0.001$, ANOVA). Looking at the different montages, significantly different LFC latencies were observed in patients 3 and 4 ($p < 0.001$, ANOVA), HFC latencies in patients 2 ($p = 0.025$) and 4 ($p < 0.001$) and VHFC latencies in patient 3 ($p < 0.001$). However, there was no clear increasing or decreasing pattern when correlating to montage distance from the tip of the electrode (see **Supplementary Ta******ble 3**).

4. Discussion

To the best of our knowledge, this is the first study to examine properties of median nerve somatosensory evoked potentials recorded from *segmented* leads in the sensory thalamus. We were

Fig. 3. Directional recordings of somatosensory evoked potential (SEP) amplitudes correlated with anatomical structures: Left: Axial view of the reconstructed electrode artifact projected onto the Morel stereotactic human brain atlas. The intersection of each slide was located in the middle point between the two levels with directional contacts of the electrode. The arrow indicates the spatial orientation of each corresponding segmented electrode. Individual directions of each contact (2–5, 3–6, 4–7) were determined using postoperative fluoroscopy to identify the orientation of the radio-opaque marker. Using patient specific fibertracking, the position of the medial lemniscus (violet and yellow) was correlated in relation to the ventral posterior thalamus. Corresponding SEP signals are shown on the right side and are connected to each directional contact. Patient 1 (A, B) and 2 (C, D) show a slightly deeper electrode implantation compared to patient 3 (E, F) and 4 (G, H). Right: Low frequency components (red), and high frequency components for the three bipolar montages (2–5, 3–6, 4–7) of each patient. In all patients, the highest SEP amplitude was recorded from the directional contacts 3–6. We found a qualitative correlation between the directional orientation of individual contacts with the highest SEP amplitude and the bulk of the medial lemniscus only in patient 1 (A, B), whereas in patient 2 (C, D), 3 (E, F) and 4 (G, H), the highest SEP amplitude did not correlate with the anatomical projection of the medial lemniscus.

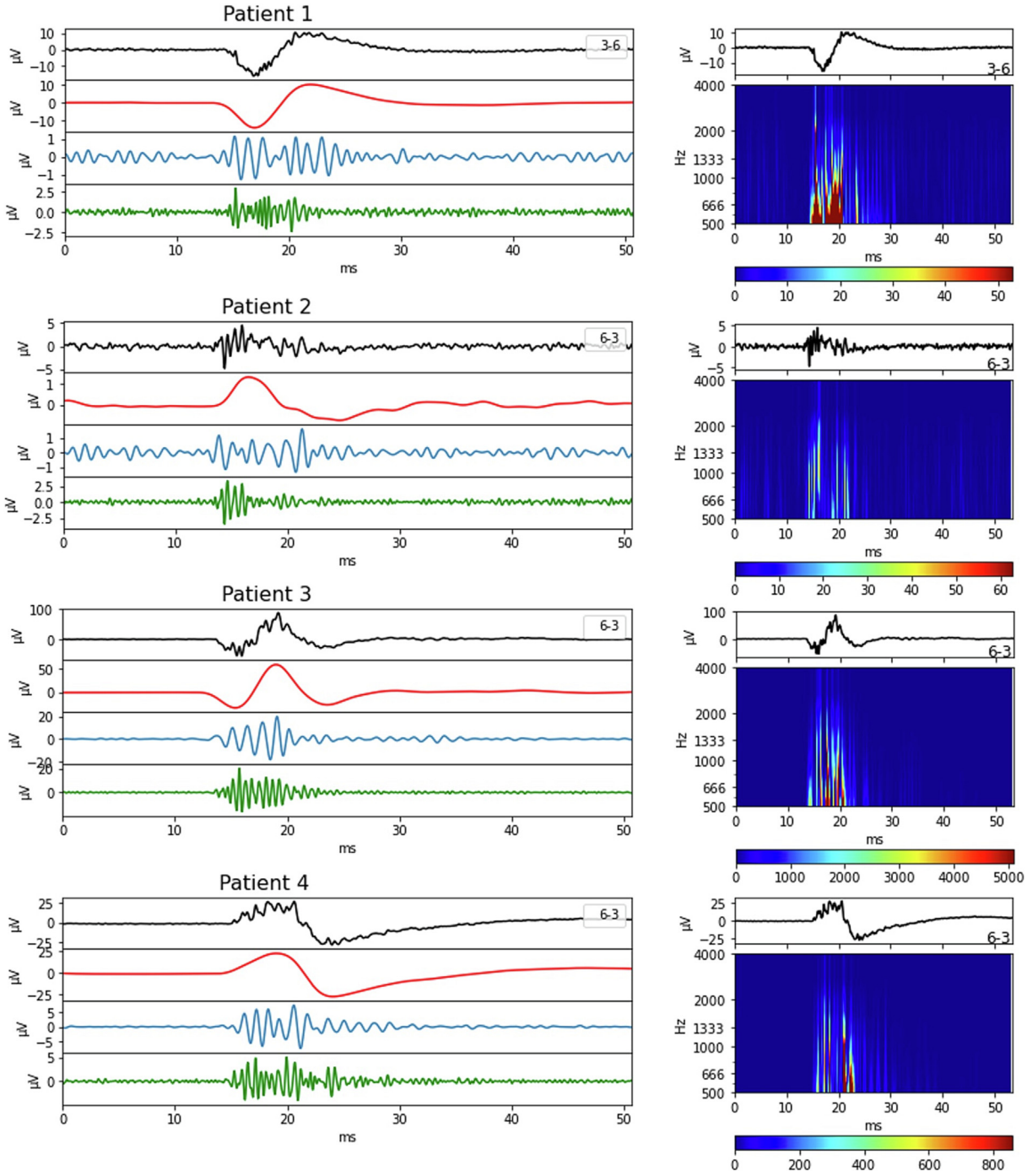

Fig. 4. Shape of low (LFC), high (HFC), and very high frequency components (VHFC) and scalograms. On the left: examples of raw signal (black), low frequency components (LFC, 20–300 Hz) (red), high frequency components (HFC, 500–1200 Hz) (blue) and very high frequency components (VHFC, 1200–5000 Hz) (green) in the best contact for each patient. On the right: scalograms of the raw signal, limited to the high and very high frequency component band. The intensity of the color relates to the energy of the signal at a certain frequency. Please note the different scales.

able to demonstrate the feasibility to carry out directional recordings of SEPs in the sensory thalamus. Amplitudes of SEPs recorded from adjacent directional electrodes differed and showed one predominant direction. Among others, Hanajima et al. recorded SEP from DBS electrodes in response to median nerve stimulation to indicate which contacts are closest to the hand sensory area and which contacts lie above or below this optimal site (Hanajima et al., 2004b). (Hanajima et al., 2004b). Our findings point to a clear directional effect and may confirm the somatotopy of the sensory thalamus. Of note, directional electrodes with the highest SEP amplitudes yielded the lowest threshold to induce paresthesia upon postoperative clinical testing. Furthermore, the spatial orientation of directional SEP amplitudes did neither match the location of the electrodes with reference to atlas-based anatomical subparcellation of the sensory thalamus nor the spatial relationship to fiber-tracking results of the medial lemniscus. Thus, the reconstructed anatomical position and spatial orientation of a directional DBS electrode does not necessarily correlate with the neurophysiological sweet spot. Hence, median nerve SEP recorded from segmented DBS leads constitute a complimentary clinical tool

to gather information about the neurophysiological (re)organization of the sensory thalamus beyond anatomical mapping data in patients with chronic pain.

4.1. Properties of SEP and high frequency oscillations

In awake patients, the **VP** is customarily identified by response to light touch or the presence of paresthesia from electrical stimulation (Obwegeser et al., 2000; Wu et al., 2014). In general, during DBS surgery of the **VP** under general anesthesia, SEP can be recorded either from the DBS lead or from microelectrode recordings (MERs) (Hanajima et al., 2004a, 2004b; Katayama and Tsubokawa, 1987). In our study, we solely applied the former method. In the **VP** response to median nerve stimulation at least two components have been described: a low frequency component (LFC) and a very high frequency component (VHFC) of approximately 1–1.5 kHz (Hanajima et al., 2004b; Klostermann et al., 2002, 2000). VHFCs have been claimed to be generated by thalamo-cortical projection neurons and were proposed as a landmark for the **VP** nucleus (Klostermann et al., 2000; Shima et al., 1991; Yamashiro et al., 1989). Vega-Zelaya et al. described another response termed high frequency oscillations (HFO), corresponding to what we call high frequency components (Vega-Zelaya et al., 2016). Later, Pastor et al. showed that HFO are more specifically detected from the **VP**, whereas VHFO were recorded also outside the **VP** (Pastor and Vega-Zelaya, 2019). We chose a different terminology than Pastor and Vega-Zelaya because we are not convinced that the (very) high frequency components of these signals really are oscillations(Luck, 2014) , since there are no lasting distinct regions of high energy in the time–frequency plots (Fig. 4). To our knowledge, we are not only the first group who describe directional recordings of LFCs and HFCs, but also who recorded LFCs and HFCs from the same electrode. Previous groups did use MER for HFC analysis and DBS electrodes for LFC analysis (Hanajima et al., 2004b; Pastor and Vega-Zelaya, 2019).

In the patient with the pure thalamic stroke, we recorded the lowest absolute SEP amplitude value. However, the HFC and VHFC amplitudes were still relatively high. This could indicate that in SEPs recorded from or near the **VP**, the LFC has a different source than the HFC and VHFC. This is supported by the fact that for patient 1 and 2, the contact of highest bipolar HFC amplitude did not correlate with the directional LFC amplitudes, whereas they did correlate for patient 3 and 4 (Fig. 2). It has to be highlighted that in patient 1 and 2 the DBS lead was implanted just below the **VP** whereas in patient 3 and 4 it is located at the exact level of the **VP** (Fig. 1).

The LFC are already generally accepted to be stationary waves from the **VP** More specifically, (Hanajima et al., 2004b) proposed thalamic SEPs recorded from the DBS electrodes in the STN result from a positive field generated by excitatory postsynaptic potentials in **VP** neurons in response to median nerve stimulation. For frequency components between 1000 – 1500 Hz, thalamocortical projections have been suggested as a source (Hanajima et al., 2004a; Klostermann et al., 2002). The latency pattern between LFC, HFC and VHFC we observed does not seem to contradict this hypothesis. One would indeed expect the (V)HFC to start later than (or at the same time as) the LFC. Looking at monopolar montage latencies, there doesn't seem to be a clear pattern, neither for HFC, nor for VHFC (**Supplementary Ta**ble 3**). If the (V)HFC were to be the result of an upward travelling wave (along the axis of the DBS lead), one would expect a latency shift: the signal should first arrive at contact 1, then 2–4, then 5–7, and lastly at contact 8. However, the geography of the pathways play a major role in shaping the measured signals which warrants further investigations into the nature and potential sources of (V)HFCs .

It should be noted that it is surprising to observe VHFC in physiological signals recorded from electrodes with a surface area in the order of a few mm^2. The area is too big to generally detect action potentials from individual neurons and the upper limit for neuron firing rate is about 1 kHz (Kandel et al., 2021). Thus, it is questionable whether the observed VHFC are the result of the same neuron population firing synchronously. Rather, one possible explanation might be that this is the result of different cell populations fire (slightly) asynchronously (which is why we chose to use (very) high frequency *components* instead of *oscillations*). In summary, the fact that LFC and (V)HFCs did not correlate in amplitude and especially directionality may be pointing towards a different source of these potentials.

4.2. Limitations

First, the low number of included patients is a limitation. In this regards, DBS to treat chronic pain patients is still rarely performed and the use of intraoperative evoked potentials is not at all routine clinical standard. Further, to improve signal analysis in the future, it would be advisable to perform baseline recordings (i.e. before the stimulus) in order to quantify the noise, as well as the changes in frequency and amplitude. Although recordings before the stimulus onset is not standard in intraoperative neurophysiology, we will implement this in the future. It would also be interesting to analyze single sweeps instead of averaged signals.

5. Conclusion

Our findings provide additional evidence for the somatotopy of the sensory thalamus. SEP recordings from directional DBS leads offer additional information about the neurophysiological (re)organization of the sensory thalamus compared to sole anatomical reconstruction of the electrodes. These signals may serve as a helpful clinical tool to identify the neurophysiological sweet spot in the sensory thalamus of patients with chronic pain. Therefore, SEPs may guide DBS lead placement and facilitate DBS stimulation parameter programming in the future.

Acknowledgements

We would like to thank Anja Giger for her graphical support of the presented figures.

Source of financial support

None.

Conflict of interest

None of the authors have potential conflicts of interest to be disclosed.

Appendix A. Supplementary data

Supplementary data to this article can be found online at https://doi.org/10.1016/j.clinph.2023.03.359.

References

Hanajima R, Chen R, Ashby P, Lozano AM, Hutchison WD, Davis KD, et al. Very fast oscillations evoked by median nerve stimulation in the human thalamus and subthalamic nucleus. J Neurophysiol 2004a;92:3171–82. https://doi.org/10.1152/jn.00363.2004.

Hanajima R, Dostrovsky JO, Lozano AM, Hutchison WD, Davis KD, Chen R, et al. Somatosensory evoked potentials (SEPs) recorded from deep brain stimulation

(DBS) electrodes in the thalamus and subthalamic nucleus (STN). Clin Neurophysiol 2004b;115:424–34. https://doi.org/10.1016/j.clinph.2003.09.027.
Kandel ER, Koester JD, Mack SH, Siegelbaum SA. Principles of Neural Science. 6th ed. McGraw Hill; 2021.
Katayama Y, Tsubokawa T. Somatosensory evoked potentials from the thalamic sensory relay nucleus (VPL) in humans: correlations with short latency somatosensory evoked potentials recorded at the scalp. Electroencephalogr Clin Neurophysiol 1987;68:187–201. https://doi.org/10.1016/0168-5597(87)90026-8.
Katayama Y, Yamamoto T, Kobayashi K, Kasai M, Oshima H, Fukaya C. Motor cortex stimulation for post-stroke pain: comparison of spinal cord and thalamic stimulation. Stereotact Funct Neurosurg 2001;77:183–6. https://doi.org/10.1159/000064618.
Klit H, Finnerup NB, Jensen TS. Central post-stroke pain: clinical characteristics, pathophysiology, and management. Lancet Neurol 2009;8:857–68. https://doi.org/10.1016/S1474-4422(09)70176-0.
Klostermann F, Funk T, Vesper J, Siedenberg R, Curio G. Double-pulse stimulation dissociates intrathalamic and cortical high-frequency (>400Hz) SEP components in man. Neuroreport 2000;11:1295–9. https://doi.org/10.1097/00001756-200004270-00030.
Klostermann F, Gobbele R, Buchner H, Curio G. Intrathalamic non-propagating generators of high-frequency (1000 Hz) somatosensory evoked potential (SEP) bursts recorded subcortically in man. Clin Neurophysiol 2002;113:1001–5. https://doi.org/10.1016/s1388-2457(02)00119-0.
Krauss JK, Lipsman N, Aziz T, Boutet A, Brown P, Chang JW, et al. Technology of deep brain stimulation: current status and future directions. Nat Rev Neurol 2021;17:75–87. https://doi.org/10.1038/s41582-020-00426-z.
Lenz FA, Garonzik IM, Zirh TA, Dougherty PM. Neuronal activity in the region of the thalamic principal sensory nucleus (ventralis caudalis) in patients with pain following amputations. Neuroscience 1998;86:1065–81. https://doi.org/10.1016/s0306-4522(98)00099-2.
Levy RM, Lamb S, Adams JE. Treatment of chronic pain by deep brain stimulation: long term follow-up and review of the literature. Neurosurgery 1987;21:885–93. https://doi.org/10.1227/00006123-198712000-00017.
Luck SJ. An Introduction to the Event-Related Potential Technique. Second Edition. The MIT Press; 2014.
MacDonald DB, Dong C, Quatrale R, Sala F, Skinner S, Soto F, et al. Recommendations of the International Society of Intraoperative Neurophysiology for intraoperative somatosensory evoked potentials. Clin Neurophysiol 2019;130:161–79. https://doi.org/10.1016/j.clinph.2018.10.008.
Macdonald DB, al Zayed Z, al Saddigi A. Four-limb muscle motor evoked potential and optimized somatosensory evoked potential monitoring with decussation assessment: results in 206 thoracolumbar spine surgeries. Eur Spine J 2007;16 (Suppl 2):S171–87. https://doi.org/10.1007/s00586-007-0426-7.
Morel A, Magnin M, Jeanmonod D. Multiarchitectonic and stereotactic atlas of the human thalamus. J Comp Neurol 1997;387:588–630. https://doi.org/10.1002/(sici)1096-9861(19971103)387:4<588::aid-cne8>3.0.co;2-z.
Nguyen TAK, Schüpbach M, Mercanzini A, Dransart A, Pollo C. Directional Local Field Potentials in the Subthalamic Nucleus During Deep Brain Implantation of Parkinson's Disease Patients. Front Hum Neurosci 2020;14. https://doi.org/10.3389/fnhum.2020.521282 521282.
Nowacki A, Zhang D, Barlatey S, Ai-Schläppi J, Rosner J, Arnold M, et al. Deep Brain Stimulation of the Central Lateral and Ventral Posterior Thalamus for Central Poststroke Pain Syndrome: Preliminary Experience. Neuromodulation 2022. https://doi.org/10.1016/j.neurom.2022.09.005.
Obwegeser AA, Uitti RJ, Turk MF, Strongosky AJ, Wharen RE. Thalamic stimulation for the treatment of midline tremors in essential tremor patients. Neurology 2000;54:2342–4. https://doi.org/10.1212/wnl.54.12.2342.
Owen SLF, Green AL, Stein JF, Aziz TZ. Deep brain stimulation for the alleviation of post-stroke neuropathic pain. Pain 2006;120:202–6. https://doi.org/10.1016/j.pain.2005.09.035.
Pastor J, Vega-Zelaya L. A new potential specifically marks the sensory thalamus in anaesthetised patients. Clin Neurophysiol 2019;130:1926–36. https://doi.org/10.1016/j.clinph.2019.07.026.
Pollo C, Kaelin-Lang A, Oertel MF, Stieglitz L, Taub E, Fuhr P, et al. Directional deep brain stimulation: an intraoperative double-blind pilot study. Brain 2014;137:2015–26. https://doi.org/10.1093/brain/awu102.
Shima F, Morioka T, Tobimatsu S, Kavaklis O, Kato M, Fukui M. Localization of stereotactic targets by microrecording of thalamic somatosensory evoked potentials. Neurosurgery 1991;28:223–30.
Vega-Zelaya L, Torres C, Sola RG, Pastor J. EP 67. Charakterization of thalamic nuclei and somatosensory evoked potentials in anesthetized humans. Clin Neurophysiol 2016;127:e203–5. https://doi.org/10.1016/j.clinph.2016.05.254.
Wu D, Wang S, Stein JF, Aziz TZ, Green AL. Reciprocal interactions between the human thalamus and periaqueductal gray may be important for pain perception. Exp Brain Res 2014;232:527–34. https://doi.org/10.1007/s00221-013-3761-4.
Yamashiro K, Tasker RR, Iwayama K, Mori K, Albe-Fessard D, Dostrovsky JO, et al. Evoked Potentials from the Human Thalamus: Correlation with Microstimulation and Single Unit Recording. Stereotact Funct Neurosurg 1989;52:127–35. https://doi.org/10.1159/000099493.